ASPECT RATIO EFFECTS ON NATURAL CONVECTION IN A RECTANGULAR CAVITY FILLED WITH HETEROGENEOUS POROUS MEDIUM

Fernando César De Lai, fernandodelai@utfpr.edu.br
Silvio L. M. Junqueira, silvio@utfpr.edu.br
Admilson T. Franco, admilson@utfpr.edu.br
Federal University of Technology - Paraná – UTFPR, Curitiba-PR 80230-901, Brazil

José L. Lage, JLL@smu.edu
Southern Methodist University – SMU, Dallas-TX 75275-0337, USA

Abstract. *In this study, the modeling and numerical simulation of natural convection process in rectangular porous cavity, heated from the side, are proposed using a microscopic approach in scale of the order of magnitude of the pores. This approach uses the heterogeneous model (or continuous) to idealize the porous medium and consists basically of two continuous phases, one is solid and the other is fluid. An idealized domain is formed by a network of pores in a solid matrix, represented by solid square blocks equally spaced, disconnected and conducting placed within a cavity filled with fluid. The aim of this study is to characterize the natural convection process in cavities filled with heterogeneous porous media for different aspect ratios. The conservation equations that model the process (mass, momentum and energy) for the solid and fluid phases, are solved numerically through the finite-volume method. Results show the effects of varying the number of blocks, the porosity of the medium, the solid-to-fluid thermal conductivity ratio and the intensification of fluid recirculation (associated to the Rayleigh number), for shallow, square and tall cavities. Investigations are carried out quantitatively in relation to the average Nusselt number of heated boundary and qualitatively by the streamlines and isotherms, characterizing the flow and heat transfer through the networks of pores. Analytical expressions are obtained to predict the phenomenon of interference between the solid obstacles and the boundary layer region, resulting from the increase of the number of blocks, the reduction of the porosity, the increase of the height of the cavity and the reduction of the Rayleigh number.*

Keywords: *Natural convection, Porous media, Heterogeneous model, Heat transfer, Aspect ratio.*

1. INTRODUCTION

Natural convection in porous media has been attracted attention of several areas of science and engineering. Nield and Bejan (1998) point various applications, such as in design and optimization of systems, civil engineering (thermal insulation of buildings and solar heating), electronics industry (packaging and cooling of cabinets), food industry (drying and storing grains), as well in the biomedical area (pulmonary breathing and capillary blood flow).

Notably in the petroleum industry, the study of heat transport and percolation in fractured formations as in well drilling and production is quite important, mainly due to the intense interaction between fluids and the formation. Such interactions, combined with the adverse environment inside the well, can lead to the invasion of drilling fluids through the fractures, eventually compromising the productivity of the drilling process. Fractured formations, associated to the most of geotechnical and hydrogeological processes, act as hydraulic conductors, as they provide a preferential pathway to the flow or, in the other way, as an obstacle to its development through the substrate.

Both the geometric and dynamic complexity, found in the transport phenomena in porous media, turn difficult to precisely analyze the various characteristics associated to such domains. To perform this task, the mathematical models proposed use micro or macroscopic approaches to represent the substrate in the pore or in the fracture scales.

The heterogeneous approach, also known in the literature as continuum model, is basically constituted of a solid and a fluid portion. Balance equations of conservation and momentum are associated to each constituent. The heterogeneous porous domain to be investigated here is a geometric simplification of a real porous medium, being represented by solid squared blocks, impermeable, disconnected, heat conductive and uniformly distributed in a squared enclosure filled with fluid. Such idealization describes a closed domain formed by a net of connected pores (fractures) in a disconnected solid matrix (blocks), representing a microscopic scale in the order of magnitude of the pores.

One of the first investigations related to this issue is due to House *et al.* (1990), which studied the thermal conductivity effects on the natural convection in a cavity containing a single, centered block. Merrikh and Mohamad (2001) were the first to analyze the effects caused by the presence of multiple blocks inside a rectangular cavity, mainly approaching both the geometric arrangement and the thermal conductivity influence over the convective transport inside the enclosure, associating these effects to the interference of the solid obstacles over the buoyancy effects present in the heated walls. Their observations were supported by the work of Merrikh and Lage (2005), as the latter considered, in addition, the effect of the variation of the number of blocks, providing a comprehensive parametric analysis for the behavior of the convective process over the interference event, as well as an analytical prediction for the minimum

number of blocks, necessary to the existence of this interference. Similar study was performed by Braga and de Lemos (2005), in which a comparison between the performance of the heterogeneous (continuum or microscopic) and homogeneous (macroscopic) approaches was conducted, in a cavity subjected to the process of both laminar and turbulent natural convection. Work of De Lai *et al.* (2008) investigates, for the first time, the effect caused by the porosity variation associated with the number of blocks over the natural convection in a heterogeneous porous medium. Extensions of their results were presented in De Lai *et al*. (2009), which show the parametric analysis for the effect of simultaneous variation of thermo-hydraulic properties of the heterogeneous model. Also, a prediction for the minimum porosity, necessary to observe the interference of the blocks over the buoyancy region, was presented.

In order to complement these studies, the present work proposes to model and simulate numerically the natural convection process in rectangular cavities, heated from the side and filled with non homogeneous porous medium. The study focuses the variation on the cavity aspect ratio ($A = L / H$). The effect of the variation of the number of blocks (N), the porosity (ϕ), the solid-to-fluid thermal conductivity ratio (K) and the fluid recirculation (associated to the Rayleigh number, Ra) for shallow ($A > 1$), square ($A = 1$) and tall ($A < 1$) cavities are analyzed using isolines (velocity and temperature) and the average Nusselt number of the heated boundary. Analytical expressions, to predict the interference of the blocks over the boundary layer, usually observed in the heterogeneous approach, are presented as well. These results form a useful reference for characterization and obtaining synthetic porous media.

2. HETEROGENEOUS MODEL: EQUATIONS AND BOUNDARY CONDITIONS

Figure 1 schematically represents an idealization of the substrate found in oil and natural gas reservoirs, in which both the geometrical complexity common to porous media and the different scales in the representation of a porous domain (Figs. 1.b and 1.c) can be observed. Such highly non-uniform geometry turns the numerical simulation a difficult task to accomplish, mainly due to the computational effort required to solve the non-linear equations. The representation of the heterogeneous porous domain is simplified and the non-dimensional boundary conditions, to be used in the mathematical formulation and in the numerical simulations, are presented in Fig. 1.d.

The cavity aspect ratio is $A = L / H$, being L the horizontal length and H the height of the cavity; U and V the non-dimensional velocity components in the X and Y directions, respectively. The left wall of the enclosure is isothermally heated (θ_H) and the right one is cooled ($\theta_C < \theta_H$). Both the bottom and the top surfaces are kept adiabatic, so $\partial\theta / \partial Y = 0$ and gravity acceleration g acts in the vertical direction. The presence of the horizontal thermal gradient applied in the vertical walls is responsible for the imbalance between buoyancy and viscous forces.

In the present study, the heterogeneous approach represents a microscopic scale at the pore magnitude, in which two constituents, the solid and the fluid, are considered homogeneous and isotropic.

The solid and the fluid proportion inside the cavity is represented by the porosity, defined as $\phi = \Delta V_f / \Delta V_T$, and related to the geometric parameters N , A and D (non-dimensional length of the blocks), being ΔV_f and ΔV_T , respectively, the volume of fluid and the total volume of the enclosure.

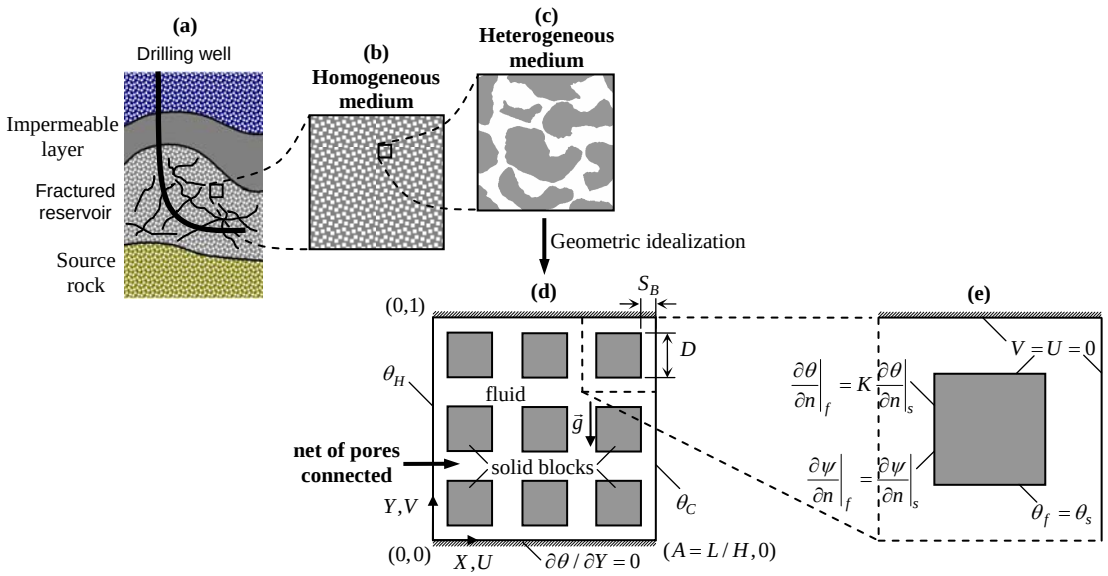

Figure 1. (a) schematic representation of a real reservoir; (b) macroscopic scale of the pore; (c) microscopic scale of the pore; (d) geometric idealization of the heterogeneous model and boundary conditions; (e) detail of the solid-fluid interface conditions.

In the balance equations formulation of the heterogeneous model, the assumptions are bi-dimensional geometry, steady state conditions. The flow is considered laminar, incompressible and monophase. The fluid is assumed as Newtonian, without viscous dissipation, with constant properties, except for the buoyancy term of Eq. (4). The density variation of the fluid is modeled by the Boussinesq approximation (Nield and Bejan, 1998), which is a suitable approach in dealing with natural convection problems.

As mentioned early in this text, according to the heterogeneous model, the balance equations consider the solid and the fluid domains separately. The momentum equation is solved in the fluid portion and the energy equation regards both the solid blocks and the network of pores filled with fluid. Therefore, the dimensionless equations for the microscopic approach can be obtained using the following relations:

$$(X,Y)=\frac{(x,y)}{H};\quad (U,V)=\frac{(u,v)H}{\alpha_f};\quad \tau=\frac{t\,\alpha_f}{H^2};\quad P=\frac{p\,H^2}{\rho_f\,\alpha_f{}^2};\quad \theta=\frac{T-T_C}{T_H-T_C} \tag{1}$$

where α_f is the thermal diffusivity of the fluid, p is the pressure and ρ_f the fluid specific mass.

The balance equations of mass, momentum (X and Y directions) and energy can be written in dimensionless form:

$$\frac{\partial U}{\partial X}+\frac{\partial V}{\partial Y}=0 \tag{2}$$

$$U\frac{\partial U}{\partial X}+V\frac{\partial U}{\partial Y}=-\frac{\partial P}{\partial X}+Pr\left(\frac{\partial^2 U}{\partial X^2}+\frac{\partial^2 U}{\partial Y^2}\right) \tag{3}$$

$$U\frac{\partial V}{\partial X}+V\frac{\partial V}{\partial Y}=-\frac{\partial P}{\partial Y}+Pr\left(\frac{\partial^2 V}{\partial X^2}+\frac{\partial^2 V}{\partial Y^2}\right)+Ra\,Pr\,\theta \tag{4}$$

$$\text{fluid: } U\frac{\partial \theta}{\partial X}+V\frac{\partial \theta}{\partial Y}=\frac{\partial^2 \theta}{\partial X^2}+\frac{\partial^2 \theta}{\partial Y^2} \tag{5}$$

$$\text{solid: } 0=\frac{K}{\sigma}\left(\frac{\partial^2 \theta}{\partial X^2}+\frac{\partial^2 \theta}{\partial Y^2}\right) \tag{6}$$

In the above equations, the following non-dimensional groups are identified: the Prandtl number, Pr, the Rayleigh number, Ra, the solid-to-fluid heat capacity ratio, σ, and the solid-to-fluid thermal conductivity ratio, K.

$$Pr=\frac{\nu_f}{\alpha_f};\quad Ra=\frac{g\beta H^3(T_H-T_C)}{\nu_f\alpha_f};\quad \sigma=\frac{(\rho c_P)_s}{(\rho c_P)_f};\quad K=\frac{k_s}{k_f} \tag{7}$$

being ν_f the fluid kinematic viscosity, β the volumetric thermal expansion coefficient, c_P the specific heat at constant pressure and k the thermal conductivity (with subscripts f and s representing, respectively, the solid and the fluid).

In Figure 1, the boundary conditions for the heterogeneous model (Fig. 1.d) and the details of the solid-fluid interface conditions can be observed in Fig. 1.e. Therefore, the boundary conditions for the heterogeneous cavity in the dimensionless form are:

$$\text{if } X=0:\ U=V=0,\ \theta=1 \text{ and if } X=A:\ U=V=0,\ \theta=0 \tag{8}$$

$$\text{if } Y=0 \text{ and } Y=1:\ \frac{\partial \theta}{\partial Y}=U=V=0 \tag{9}$$

and at the solid-fluid interface in the solid blocks, the following boundary conditions are considered:

$$U=V=0;\quad \theta\big|_f=\theta\big|_s;\quad \left.\frac{\partial\theta}{\partial n}\right|_f=K\left.\frac{\partial\theta}{\partial n}\right|_s;\quad \left.\frac{\partial\psi}{\partial n}\right|_f=\left.\frac{\partial\psi}{\partial n}\right|_s, \tag{10}$$

being n the unit vector perpendicular to the surfaces of each block.

Solution of Equations (2)-(6) is performed by means of the control volume method using SIMPLEST algorithm (Patankar and Spalding, 1972) for the pressure-velocity coupling. The hybrid scheme is applied to interpolate the advective terms. Convergence is achieved whenever the sum of the absolute values of the local residue, of each variable (U, V, P and θ), between two consecutive iterations is less than 1×10^{-6}.

The streamfunction ψ defined by Eq. (11) satisfies the Eq. (2) that represents the mass balance (Kimura and Bejan, 1983). The numerical values of the streamlines are obtained and shown in module for the lowest value found inside the cavity, $|\psi|$. In the solid walls of the cavity $\psi = 0$.

$$\psi = \psi_{i,j} = \psi_{i,j-1} + \int_{Y_{j-1}}^{Y_j} U_{i,j}\, dY = \psi_{i-1,j} + \int_{X_{i-1}}^{X_i} -V_{i,j}\, dX \tag{11}$$

The dimensionless average temperature gradient, which permits to quantitatively analyze the convective heat transfer in a surface, regardless its coordinate, is defined as $Nu_{av} = h_{av} H / k_f$. The heat transfer in the enclosure is described by the estimation of Nu_{av} at the heated wall. Due to the steady and adiabatic conditions at the bottom and top surfaces, Nu_{av} must present the same value for the hot and the cooled walls.

$$Nu_{av} = \frac{h_{av} H}{k_f} = -\int_0^1 \left.\frac{\partial \theta}{\partial X}\right|_{X=0} dY \tag{12}$$

where the averaged heat transfer coefficient, h_{av}, is estimated by the expression $h_{av} = q''_{av} / (T_H - T_C)$, being the heat flux at the heated wall given by $q''_{av} = -k_f (\partial T / \partial x)_{av:h}$.

3. RESULTS AND DISCUSSION

For the proposed model, results are presented for the effect of changes in the values and parameters of Tab. 1. To solve equations (2) to (6), unit values for σ and Pr are considered. To investigate the simultaneous variation of the thermo-hydraulic properties the familiarization with some geometric characteristics of the cavity is necessary. Porosity ϕ remains constant even if N increase, as the geometric parameter D is reduced. However, to investigate the variation of ϕ, D must be reduced as ϕ increase, for a certain N. That means the determination of D is important to construct the heterogeneous cavity, which is obtained for a given configuration of N and ϕ, through the expression $D = [(1-\phi)/N]^{1/2}$, where $(1-\phi)$ represents the solid fraction.

Table 1. Parameters and values to characterize the heterogeneous model investigated.

A	0.25; 0.5; 1; 2; 4
Ra	10^5; 10^6; 10^7; 10^8
N	$1\times g_B$; $9\times g_B$; $16\times g_B$; $36\times g_B$
K	0.1; 1; 10; 100
ϕ	0.36; 0.51; 0.64; 0.75; 0.84

For varying the parameter A (Fig. 2), ϕ is arbitrated as a constant, due to better interpretation and comparison of the results, instead of using the parameter N. Therefore, the idea of the group of blocks, g_B, is introduced to preserve the porosity even when varying the cavity aspect ratio, A.

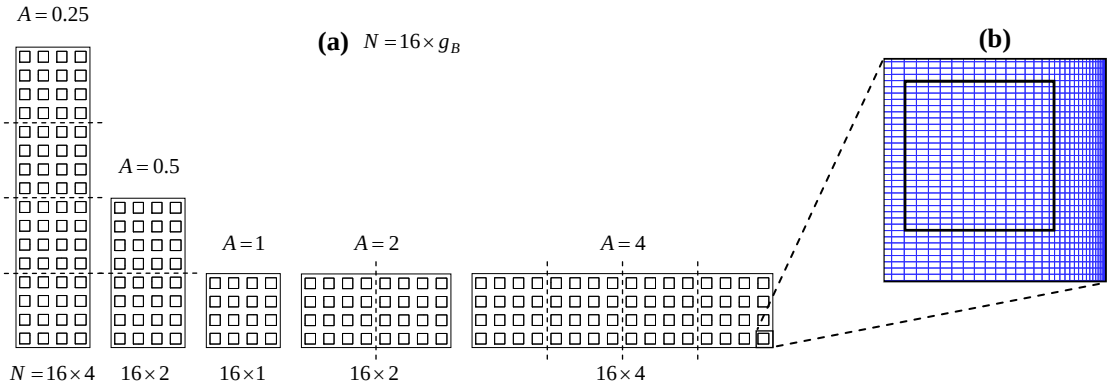

Figure 2. (a) Variation of A: number of groups of blocks in the vertical ($g_B = A^{-1}$), for tall cavity ($A < 1$), and the horizontal ($g_B = A$), for shallow cavity ($A > 1$); (b) Detail of non-uniform computational mesh.

Figure 2.a exemplifies the repetition of pattern of blocks in the vertical (tall cavity) and the horizontal (shallow cavity) directions, by varying A for configurations with $N = 16 \times g_B$. If a squared cavity ($A = 1$), with a group of 16 blocks ($N = 16 \times 1$) has its configuration changed to $A = 2$, another group of blocks is introduced in the horizontal direction ($N = 16 \times 2$), so the porosity remains constant in both configurations. Therefore, the number of group of blocks, g_B, can be identified in terms of the aspect ratio, A. For higher cavities ($A < 1$), $g_B = A^{-1}$ and the group of blocks is repeated in the vertical. On the other hand, when the cavity is wide, $A > 1$ and $g_B = A$, as the group of blocks is horizontally repeated.

Figure 2.b shows in detail the non-uniform computational grid applied in regions near the isothermally heated walls. The refinement observed is based on the boundary layer thickness of the vertical walls, which varies according to the Rayleigh number Ra and the cavity height H.

The validation of both the methodology and the numerical code were achieved by comparison with two classic configurations found in literature, as observed in Tables 2 and 3. Results for the cavity filled with clear fluid (Table 2) and cavity with a single centered conductive block (Table 3) are shown. The proximity between the results gives credibility to the numerical modeling here presented, in dealing with the natural convection in heterogeneous domain.

Table 2. Nu_{av} : validation for the cavity with clear fluid.

Ra	Kalita *et al.* (2001) *Pr* = 0.71	Merrikh and Lage (2005) *Pr* = 0.71	Braga and de Lemos (2005) *Pr* = 1	[present] *Pr* = 1
10^4	2.245	2.244	2.249	2.258
10^5	4.522	4.536	4.575	4.605
10^6	8.829	8.860	8.918	8.992
10^7	16.520	16.625	16.725	16.890
10^8	-	31.200	30.642	31.048

Table 3. Nu_{av} : validation results for single block cavity.

Ra	*D*	*K*	Bhave *et al.* (2006) *Pr* = 0.71	Merrikh and Lage (2005) *Pr* = 0.71	House *et al.* (1990) *Pr* = 0.71	[present] *Pr* = 0.71
10^5	0.5	0.2	4.645	4.605	4.624	4.625
10^5	0.5	5.0	4.338	4.280	4.324	4.320
10^6	0.9	0.2	2.326	2.352	2.402	2.415
10^6	0.9	5.0	-	-	3.868	3.810

3.1. Boundary layer interference

For problems involving microscopic approaches, the geometric effect due to the presence of solid obstacles, provides significant variation in the behavior of the flow and the heat transfer within the enclosures. In the present work, this effect can be analyzed and considered mainly in the distance between the first column of blocks and the walls of the enclosure, S_B, as depicted in Fig. 1.d.

As mentioned before, when increasing the number of blocks (N) is necessary to reduce the dimensionless length of blocks (D), for the porosity of the cavity (ϕ) remains constant. This increase of N makes the blocks get closer to the walls, occupying the regions of boundary layer, providing an abrupt change in the preferential flow path and the heat transfer inside the cavity due to the significant effect of the solid interfaces. Therefore, is reasonable to assume the existence of a minimum number of blocks, N_{min}, for which higher values of N, the flow is affected in a more pronounced way. Thus, the preferential flow path, adjacent to the walls, tends to move to the first vertical channel located between the two consecutive columns of blocks, as pointed by Merrikh and Lage (2005). Analogously to the conception of N_{min}, it is possible to foresee a minimum porosity, ϕ_{min}, for which the transport of fluid and energy in the enclosure are more sensible as a consequence of elevating the solid fraction or decreasing ϕ, as concluded by De Lai *et al.* (2009). Such interference can be analytically predicted, by comparing the boundary layer scale for the natural convection, S_C, with the distance from the heated (or cooled) wall to the solid blocks, given by $S_B = [1-(1-\phi)^{1/2}]/(2N^{1/2})$. For $Pr \geq 1$ and just one heated wall, the scale that represents better the boundary layer thickness is $H\,Ra^{-1/4} \sim S_C/2$ (Nield and Bejan, 1998). The interference of the obstacles over the buoyancy region, as a result of increasing N or decreasing ϕ, is expected when $S_B < S_C$. By using the ratio between S_B and S_C, written in terms of Ra, N, ϕ and H, it is possible to obtain predictions of N_{min}, Eq. (13.a), and ϕ_{min}, Eq. (13.b). Table 4 shows the predictions of N_{min} for each configuration of Ra and A, for $\phi = 0.64$.

$$\text{(a)}\ N > \frac{[1-(1-\phi)^{1/2}]^2}{16\,H^2} Ra^{1/2}\ ; \quad \text{(b)}\ \phi < 1-\left(1-\frac{4H\,N^{1/2}}{Ra^{1/4}}\right)^2 \tag{13}$$

Notice that the prediction of N_{min} when $A \geq 1$ occurs for the same values of N, as the length H for those configurations remains constant. Still in Table 4, the absence of N_{min} for $Ra = 10^5$ and $A = 0.25$, means that the ascendant boundary layer (heated wall) and the descendant boundary layer (cooled wall) interfere on each other, not depending on the existence of blocks inside the cavity.

Table 4. Prediction of $N_{min} = f(Ra, H, \phi)$, Eq. 13.a, for $\phi = 0.64$.

Ra	A		
	0.25	0.5	1; 2; 4
10^5	-	1	3
10^6	1	3	10
10^7	2	8	32
10^8	6	25	100

3.2. Effect of thermo-hydraulic properties

Results achieved using the heterogeneous approach are analyzed regarding the predictions of N_{min} and ϕ_{min}, due to the behavior of the transport of fluid and heat, which varies according to the displacement of the obstacles in the cavity, as well as the variation of its thermo-hydraulic properties.

As discussed earlier, the placement of the blocks inside the enclosure, can act in a way more or less significant to the flow development and, consequently, in the heat transfer, due to its interference on the boundary layers of the isothermal walls.

In Figure 3 graphs of Nu_{av} versus N (a1; b1) and versus ϕ (a2; b2) are presented for $Ra = 10^6$, regarding four values of K. Curves of N_{min} - Eq. (13.a)- and ϕ_{min} - Eq. (13.b)- are depicted to bound the configurations presenting the interference in the boundary layer. The dispersion in the K curves, observed when $N > N_{min}$ or $\phi < \phi_{min}$, is intensified as N increases or ϕ is reduced. For $N > N_{min}$, the increase of K implies in higher values of Nu_{av} (a1; b1), for N constant. In the other way, when $N < N_{min}$, the increase of K provokes no significant variation in Nu_{av}. In Figure 3 (a2; b2), the higher is ϕ, distinct behaviors due to the K curves can be observed in the values of Nu_{av}. In general, for $K < 1$, the increase of ϕ (a2; b2) strengthens the heat transfer process (Nu_{av} increases). When $K > 1$, the heat transfer can be dampened as ϕ is raised, possibly due to the competitive effect of $K > 1$ in configurations where the conduction is more pronounced than the convection, as in cases of low Ra and higher values of N. That can be noticed in Fig. 3.b2, for $K = 10$ and $K = 100$. In addition, the reduction of the conduction effect (Fig. 3.b2), when the convective transport starts to become more important as ϕ increases, as shown in Fig. 3.a2, as N was reduced to 9. As a remark, cases where $\phi > \phi_{min}$, meaning that no interference in the boundary layer is verified, steepened values of K provoke no significant variations in Nu_{av} (see that Fig. 3.a2 indicates the absence of the interference when $\phi > 0.61$).

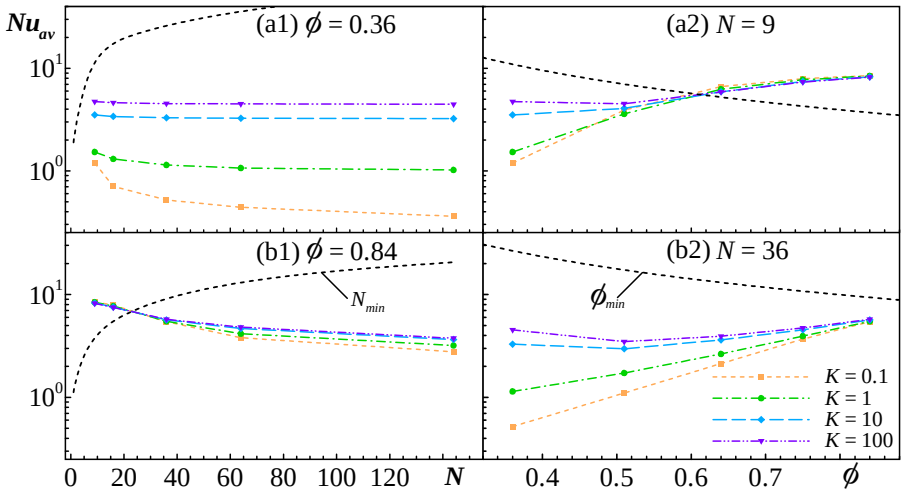

Figure 3. Nu_{av} versus N (a1; b1) and ϕ (a2; b2) for $Ra = 10^6$.

In Figure 4 (left side), a graph of Nu_{av} versus $N \times g_B$ is presented for each configuration of A, where the curves are set for each Ra, along with the curve of N_{min}, Eq. (13.a), that delimitate those configurations presenting the interference regarding the variation of N. The curves of $Ra = 10^5$ present in Figure 4 confirm the limit for Nu_{av} as N is increased. Such limit can be interpreted as a pure conduction regime, commonly observed in cases of low Ra and high N. For those configurations predominantly conductive, one can associate Nu_{av} with the cavity aspect ratio through the expression $Nu_{av} \sim A^{-1}$. On the right side of Figure 4, the streamlines for the some cases of $N \times g_B$ for $Ra = 10^7$, $\phi = 0.64$ and $K = 1$ are presented, concerning the variation of the aspect ratio A, just aiming to identify the changes in the flow configuration as N increases, and in the same sense, to verify the transition of those configurations where the interference can be observed.

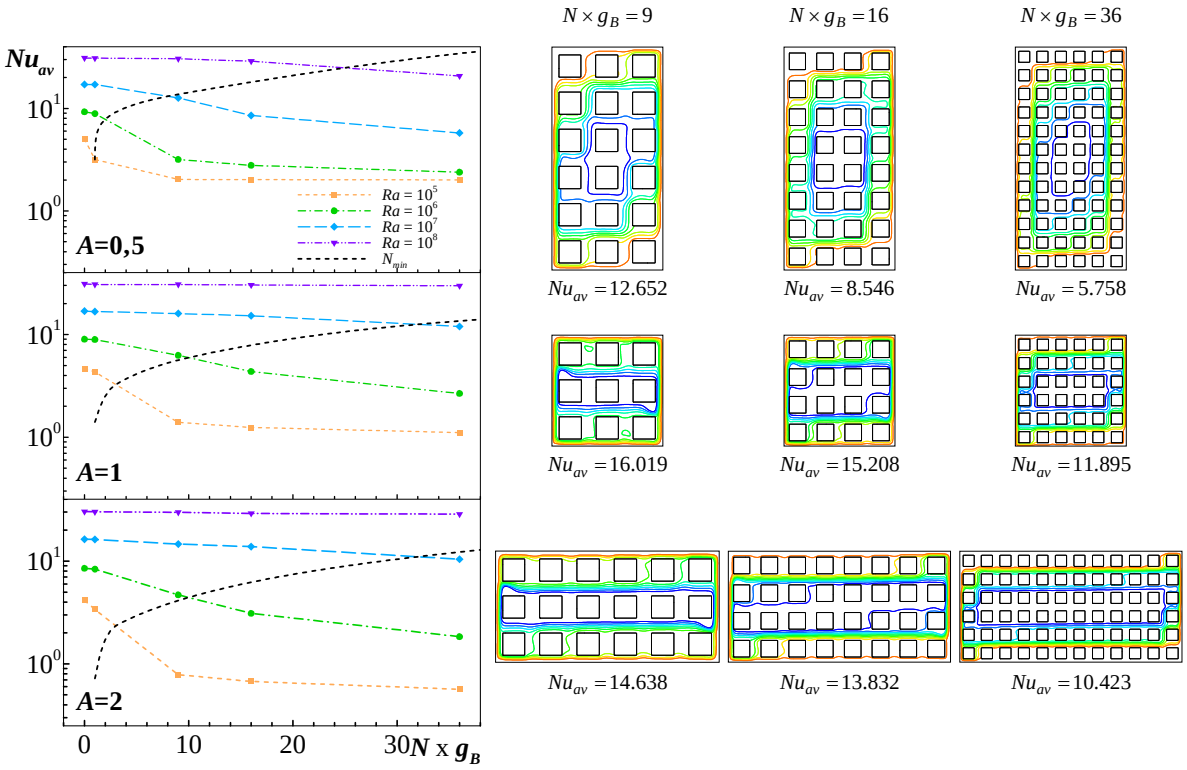

Figure 4. On the left: Nu_{av} versus N (prediction of N_{min}, Eq. 13.a, for $\phi = 0.64$);
and on the right: streamlines for various N and A, for $Ra = 10^7$, $\phi = 0.64$ and $K = 1$.

In the isolines of Figure 4, it can be noticed that raising the values of A from 0.5 to 1, increases the Nu_{av}. That is due to the reduction of the boundary layer region, which weakens the interference of the blocks. An opposite effect (reduction of Nu_{av}) is observed if the value of A is raised from 1 to 2, since those configurations present the same cavity height (H), and by consequence, the same boundary layer thickness (S_C). Thus, the raise of A increases L, as well the resistance to the flow path.

The boundary layer interference phenomenon, that increases with N, is verified in the graphs of Fig. 4, as the Nu_{av} is reduced right above the curve of N_{min}. This event is characterized by the change in the preferential flow path in the cavity, as observed in the streamlines. In general, for $N < N_{min}$, the preferential flow is adjacent to the isothermal walls; and when $N > N_{min}$ the flow path turns to the first vertical channel between the two columns of blocks. For $A = 0.5$ such change in the fluid flow path is expected if $N > 8 = N_{min}$, and becomes more evident as N increases. When $A = 1$, for which $N_{min} = 32$, the change in the flow can be verified when $N = 36$. For those configurations with no interference ($N < 32$), the preferential flow is adjacent to the isothermal walls. Observe that for $A = 2$ the prediction for N_{min} remains the same as the estimated in the case $A = 1$.

These analysis are complimentary with the results of Figure 5, that show the effect of the aspect ratio (A) variation over the average Nusselt number Nu_{av}, according to different $N \times g_B$ curves, for a range of Ra. Notice that the $N \times g_B = 0$ curve shows the Nu_{av} in terms of A, regarding a clear fluid cavity. Indeed, the $N = 0$ curves serve to delimit a threshold for the heat transfer, if compared with configurations that present solid obstacles inside the cavity.

In Figure 5.a ($Ra = 10^5$, $\phi = 0,64$ and $K = 1$), a tendency to reduction of Nu_{av} can be observed as A increases, characterizing a possible connection between the interference phenomenon and the conductive process in the cavity. Nevertheless, for $N \times g_B = 1$, the increase of A implies in changes in Nu_{av} that do not follow the pattern observed in the other configurations of $N \times g_B$. Increasing A from 0.25 to 0.5, a reduction in Nu_{av} occurs, since both configurations present the interference phenomenon. On the other way, raising A from 0.5 to 1, in which $N_{min} = 3$, the value of Nu_{av} increases as well, since there no interference on the boundary layer when $A = 1$.

An intensification in the flow recirculation and temperature gradients comes out with the increase of Ra, as well the narrowing of the boundary layer. In Figure 5.b ($Ra = 10^6$, $\phi = 0.64$ and $K = 1$) it is observed that for $N \times g_B = 1$, only the configuration of $A = 0.25$ present the interference on the boundary layer. Thus, there is an increase of Nu_{av} when compared with $A = 0.5$. For $N \times g_B > 1$ there is a transition in the tendency of Nu_{av}, that for $A = 0.25$ to $A = 0.5$ presents a reduction of Nu_{av} due to reduction of H and especially for the competitive effect between the interference phenomenon and the intensity of the magnitude of the boundary layer. This effect is better visualized for $N \times g_B = 16$, that even for configurations of $A = 0.5$ and $A = 1$ presenting the interference on the boundary layer, the increases in A resulting in an increasing of Nu_{av}, due to the higher effect of the convective process in the cavity for

$A=1$ that for $A=0.5$. Note that when $N \times g_B$ is increased to 36 there is an increase in the conductive process due to the increase of solid obstacles in the flow. Consequently, there is an interference effect in the boundary layer more significantly, causing an attenuation in the increase of Nu_{av} according to the increase of $A=0.5$ to $A=1$. From $A=1$ to $A=4$ is observed the reduction tendency of Nu_{av}, previously observed by the increase of L.

In Figure 5.c ($Ra=10^7$, $\phi=0.64$ and $K=1$) is more evident the competitive effect between the interference of the blocks with the intensity of recirculation flow. For $N \times g_B=1$ observed that the value of Nu_{av} is practically the same as for the clear cavity. As $N \times g_B$ is increased it is possible to observe the tendency of Nu_{av} with the increasing of A, that unlike $0.25 \le A \le 1$ configurations with $1 \le A \le 4$ show a tendency of Nu_{av} for a given N, due to the same boundary layer thickness S_C. It is observed with increasing A the reduction of Nu_{av} due to the increase of length L, that increases the distance between the isothermal walls, hindering the heat transfer and recirculation flow, presenting a more significant manner as N is increased.

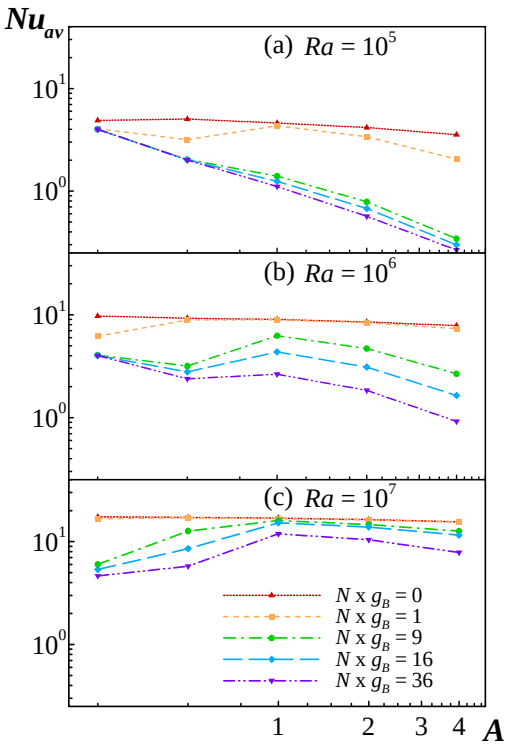

Figure 5. Nu_{av} versus A for $\phi=0.64$ and $K=1$: (a) $Ra=10^5$, (b) $Ra=10^6$ and (c) $Ra=10^7$.

Figure 6, for $Ra=10^5$ and $N=36 \times g_B$, shows the isotherms (a) and the streamlines (b) for the configurations where the conductive process is dominant, the evolution of the isolines, as well the values of Nu_{av} can be observed for all aspect ratios. The vertical stratification of the isotherms (Fig. 6.a) and the small magnitude of fluid recirculation through the cavity characterize the conduction dominant process. That can be confirmed by observing the uniformity of the streamline profiles (Fig. 6.b). These observations are corroborated by the results of Fig. 4 (left), which shows Nu_{av} values varying with A, Ra and N, where the tendency to the pure conduction limit can be noticed in Nu_{av} values, for low Ra and high N. Thus, the presence of solids in the buoyancy region is evident when $N > N_{min}$, which significantly influences the reduction of Nu_{av} towards the conduction regime.

In opposition to those cases shown in Figure 6, the configurations considered in Figure 7 are illustrative of convection dominant situations, found in cases of high Ra and low N. Figure 7 shows the isolines when $Ra=10^8$ and $N=9 \times g_B$, with Nu_{av} values varying with the aspect ratio, A. The vertically stratified isotherms (Fig. 7.a), an indication of a convection dominant process, is confirmed by observing the high magnitude of flow circulation and also the anti-simmetry of the streamlines (Fig. 7.b).

Based on the Table 4 (prediction of N_{min}) is evident that only the configuration $A=0.25$ presents interference in the boundary layer, as for this configuration one has $N_{min}=6$. For other aspect ratios the blocks do not present any interference, and in this sense, the flow is developed adjacent to the isothermal walls. It is worth mentioning again the similarity of the evolution of the profiles of isolines (isotherms and streamlines) with the increase of $1 \le A \le 4$, precisely because the same boundary layer thickness, differing only in the extent of the isolines profile due to the increase of L.

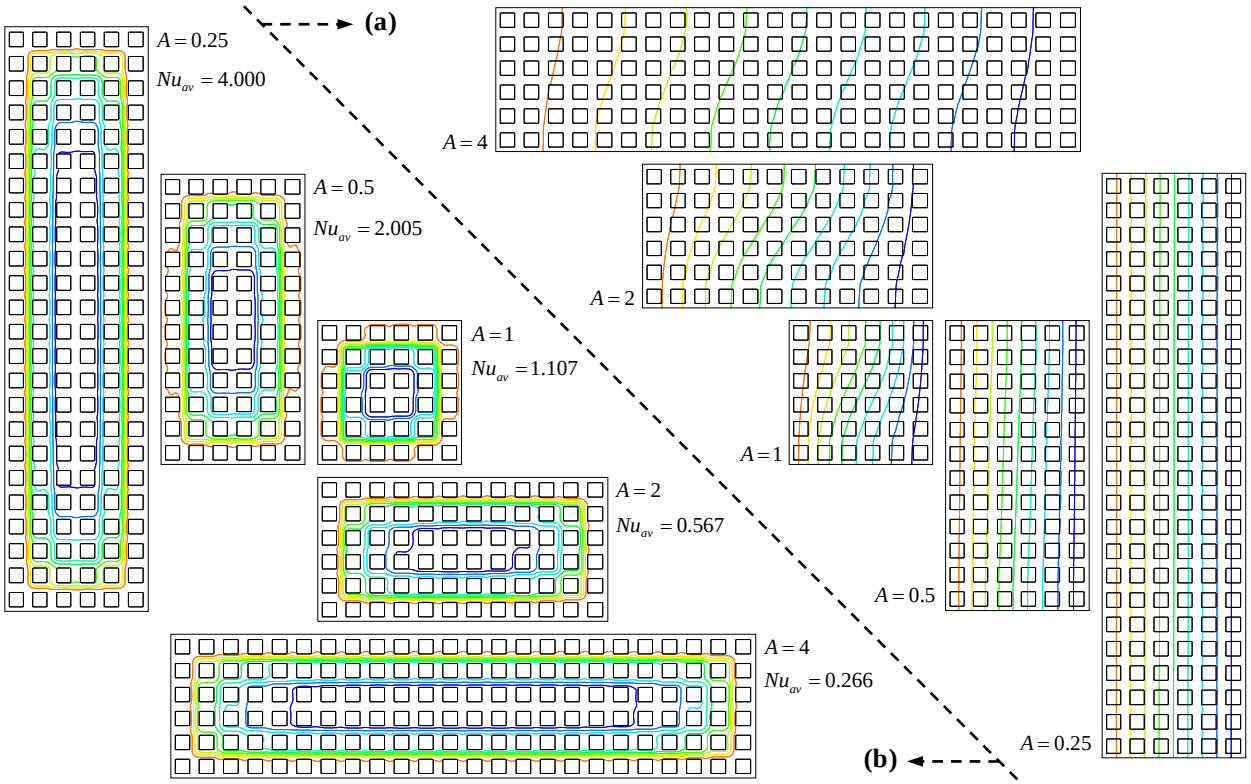

Figure 6. (a) isotherms and (b) streamlines: variation of $A = L/H$ for $Ra = 10^5$, $N = 36 \times g_B$, $\phi = 0.64$ and $K = 1$.

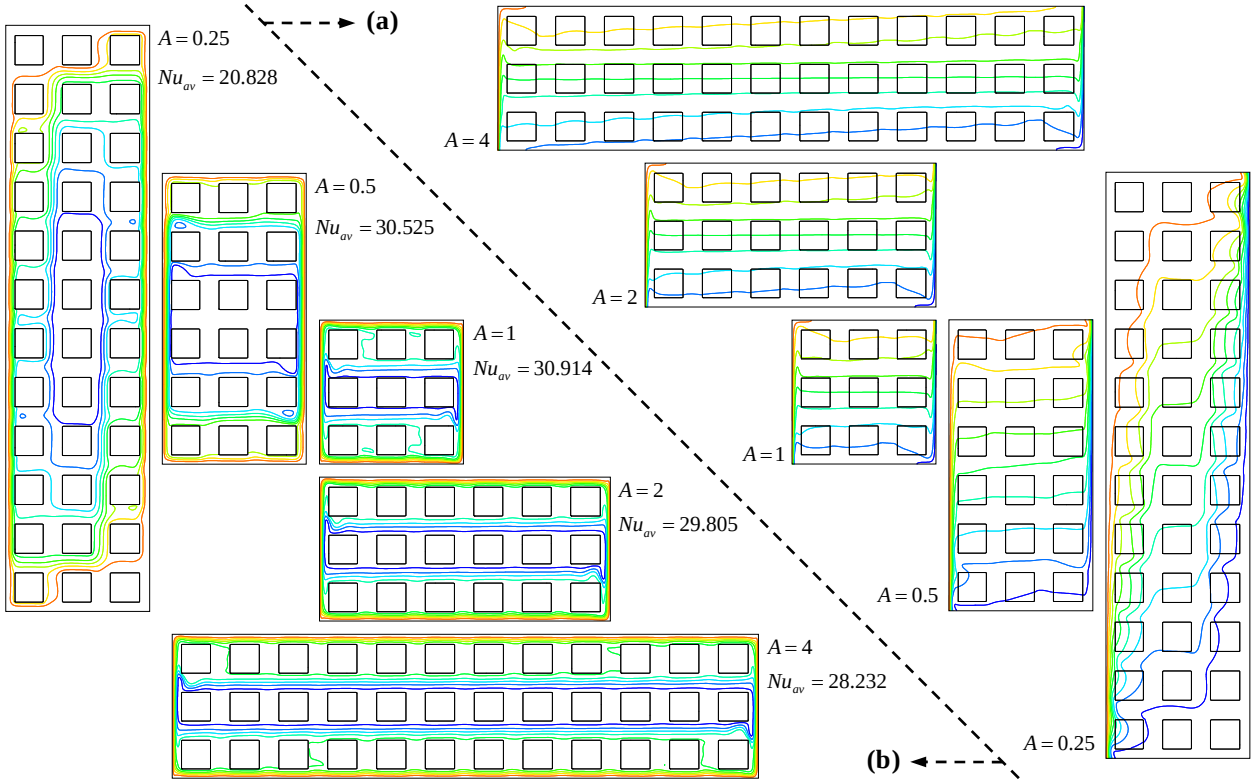

Figure 7. (a) isotherms and (b) streamlines: variation of $A = L/H$ for $Ra = 10^8$, $N = 9 \times g_B$, $\phi = 0.64$ and $K = 1$.

4. CONCLUSIONS

The natural convection process in heterogeneous cavities has been numerically analyzed to verify the influence of parameters Ra, N, K, ϕ and A. When the blocks are close to the walls, from the increase of N or reduction of ϕ,

they can eventually interfere with the boundary layers. This effect is anticipated on the basis of a scale analysis result predicting the boundary layer thickness. The analytical expressions for N_{min} and ϕ_{min} are obtained in order to predict the cases in which the change in the flow path will occur, where verified with good accuracy by numerical results. In general, for configurations without the presence of interference of the blocks on the boundary layer ($N < N_{min}$ or $\phi > \phi_{min}$), the increase of K , does not present any significant variation in Nu_{av} values. Nevertheless, for configurations where the interference can be observed ($N > N_{min}$ or $\phi < \phi_{min}$), the increase of K enhanced the heat transfer across the cavity. For $K < 1$, the increase of ϕ strengthens the process of heat transfer in the cavity, due to reduction in the proportion of solid obstacles. Depending on the magnitude of the increase in K , an augmentation in ϕ can reduce the Nu_{av} . Such occurrence is related to the prominence of conduction effect, which prevails over the convection one, provided by $K > 1$ as solid blocks are placed near the vertical walls. In the variations of the aspect ratio (A) here presented, only simultaneous effects on Ra and N are investigated, as the parameters K and ϕ remained constant. Numerical results are analyzed according to N_{min} predictions. In general, for $0.25 \le A < 1$ (tall cavity), the boundary layer thickness, $S_C = f(Ra, H)$, increases if compared to $A = 1$. For $A \ge 1$ (shallow cavity), S_C is constant and, in this case, the interference is verified always for the same value of N . In summary, as A is increased, the heat transfer presents distinct behavior regarding the presence of blocks in the boundary layer. Configurations where $N < N_{min}$, an increment of A , for a certain N , present a reduction of Nu_{av} , due the reduction of the cavity height H (in cases where $0.25 \le A \le 1$) and the increase of L (in cases where $1 \le A \le 4$). Cases in which $N > N_{min}$, an increment of a certain $A = 0.25$ to $A = 1$, point an increasing of Nu_{av} . That it is explained by the greater interference of the blocks on the boundary layer, as A is decreased. For the increase from $A = 1$ to $A = 4$, the values of Nu_{av} are reduced, as these configurations present the same values of S_C , being affected by the increase of L (the flow path is increased). In configuration where the conduction process is dominant, as in the cases of low Ra and high N , characterized a pure conduction regime. For those configurations predominantly conductive, one can associate Nu_{av} with the cavity aspect ratio through the expression $Nu_{av} \sim A^{-1}$.

5. REFERENCES

Bhave, P., Narasimhan, A. and Rees, D.A.S., 2006 “Natural convection heat transfer enhancement using adiabatic block: Optimal block size and Prandtl number effect”, International Journal of Heat and Mass Transfer Vol. 49, pp. 3807-3818.

Braga, E.J. and de Lemos, M.J.S., 2005, “Heat transfer in enclosures having a fixed amount of solid material simulated with heterogeneous and homogeneous models”, International Journal of Heat and Mass Transfer, Vol. 48, pp. 4748-4765.

De Lai, F.C., Junqueira, S.L.M., Franco, A.T., Lage, J.L., Martins, A.L. and Lomba, R.F.T., 2009, “Análise paramétrica da transferência de calor por convecção natural em cavidade com meio poroso heterogêneo”, Anais do 5º Congresso Brasileiro de P&D em Petróleo e Gás, Fortaleza, Ceará, Brasil.

De Lai, F.C., Junqueira, S.L.M., Franco, A.T. and Lage, J.L., 2008, “Natural convection through enclosed disconnected solid blocks”, Proceedings of the 12th Brazilian Congress of Thermal Engineering and Sciences, Belo Horizonte, Minas Gerais, Brasil.

House, J.M., Beckermann, C. and Smith T.F., 1990, “Effect of a centered conducting body on natural convection heat transfer in an enclosure”**,** Numerical Heat Transfer, Part A, Vol. 18, pp. 213-225.

Kalita, J.C., Dalal, D.C. and Dass, A.K., 2001, “Fully compact higher order computation of steady-state natural convection in a square cavity”, Physical Review E, Vol. 64, pp. 1-13.

Kimura, S. and Bejan, A., 1983, “The ‘heatline’ visualization of convective heat transfer”, ASME Journal Heat Transfer, Vol. 105, pp. 916-919.

Merrikh, A.A. and Lage, J.L., 2005, “Natural convection in an enclosure with disconnected and conducting solid blocks”, International Journal of Heat and Mass Transfer, Vol. 48, pp. 1361-1372.

Merrikh, A.A. and Mohamad, A.A., 2001, “Blockage effects in natural convection in differentially heated enclosure”, Journal Enhanced Heat Transfer, Vol. 8, pp. 55-74.

Nield, D.A. and Bejan, A., 1998, “Convection in porous media”, Second ed., Springer-Verlag, New York, U.S.A.

Patankar, S.V. and Spalding, D.B., 1972, “A calculation procedure for heat. mass and momentum transfer in three-dimensional parabolic flows”, International Journal of Heat and Mass Transfer, Vol. 5, pp. 1787-1806.

6. ACKNOWLEDGEMENTS

The authors are thankful to the support provided by the TEP/CENPES/PETROBRAS, the Brazilian Petroleum Agency (ANP), the Human Resources Program for the Petroleum and Gas Sector PRH-ANP (PRH10 – UTFPR) and the UTFPR Science Foundation (FUNTEF-PR).

7. RESPONSIBILITY NOTICE

The authors are the only responsible for the printed material included in this paper.